Scanning Concentration Correlation Spectroscopy using the Confocal Laser Microscope

Dennis E. Koppel, Frank Morgan, Ann E. Cowan and John H. Carson
Departmentof Biochemistry, University of Connecticut Health Center, Farmington, Connecticut 06030 USA

ABSTRACT Concentration correlation spectroscopy allows the assessment of molecular motions in complex systems. The technique generally monitors concentration fluctuations by means of some method such as the intensity of fluorescent molecules (fluorescence correlation spectroscopy). We describe here the use of scanning confocal laser microscopy to measure correlation functions in both space and time. This methodology offers two major advantages over conventional methods. First, collecting data from different regions of the sample significantly increases the signal-to-noise ratio. Second, molecular motions of colloidal gold can be analyzed by correlation methods with high temporal and spatial resolution. Using a MRC 600 laser scanning system, we collect data from an ensemble of 768 independent subvolumes and determine the space-time correlation function. We demonstrate the technique using two different types of samples, fluorescently labeled DNA molecules in solution and colloidal gold-tagged lipids in a planar bilayer. This approach, which we term "scanning concentration correlation spectroscopy," provides a straightforward means of performing high resolution correlation analysis of molecular motions with available instrumentation.

INTRODUCTION

Concentration correlation techniques allow accurate quantitation of lateral, chemical, and rotational motions of small numbers of specific molecules in complex systems (Magde et al., 1974). In the fluorescence correlation spectroscopy (FCS) technique, for example, measurements of the time correlation function of concentration fluctuations of fluorescent molecules have been used to characterize the dynamics of molecular motions (Elson and Magde, 1974; Magde et al., 1974; Koppel, 1974; Koppel et al., 1976; Qian and Elson, 1991; Thompson and Axelrod, 1983; Palmer and Thompson, 1987a, b; Petersen, 1986a, b; Petersen and Elson, 1986; Nicoli et al., 1980). Concentration fluctuations can correspond to concentration or "occupation-number" fluctuations as molecules move in and out of the observation volume or undergo chemical transformations.

FCS provides several unique advantages over fluorescence recovery after photobleaching as a means of quantitating molecular motions. In addition to measurement of diffusion coefficients and flow velocity, FCS can be used to measure particle number, aggregation states of molecules, and interactions between diffusing species. In addition, FCS analysis can also be used in principle to study chemical kinetics. Unfortunately, the need for dedicated and costly equipment and signal-to-noise limitations have precluded the use of FCS by many researchers.

In the method introduced here, the concentration correlation technique is coupled to the scanning confocal laser-microscope to provide a readily available system for collecting concentration fluctuation data from an ensemble of independent subvolumes. Correlating the signal over both time and space provides a signal-to-noise ratio improved by several orders of magnitude over that of conventional FCS. The idea of monitoring different subvolumes was employed previously by Weissman et al. (1976). By slowly rotating a sample about an axis, they provided quantitative estimates of the molecular weight of DNA in solution. Several years later, Meyer and Schindler (1988) described another instrument that used a rotating objective lens to cover a circular path on the sample. However, these approaches suffer from low resolution and the expense of building a dedicated instrument.

Petersen (1986a, b) developed a scanning FCS method to examine particle aggregation in samples in which diffusion or flow is slow. In the original method, the sample is translated relative to a stationary laser beam using a custom designed translating stage. The spatial autocorrelation function is then determined based on 30 to 50 measurements across the sample. More recently, Petersen et al. (1993) have adapted this method for use with a scanning confocal microscope, calling the method image correlation spectroscopy. In the image correlation spectroscopy method the spatial correlation function is determined for confocal microscope images in samples where diffusion is slow. Here, we have used the scanning confocal laser microscope to perform correlation analysis in both time and space. The scanning confocal laser microscope provides the ability to rapidly and repeatedly scan a single line of the sample, and thus is perfectly suited for concentration correlation analysis.

FCS relies on fluorescence labeling to detect specific molecules. The recent introduction of colloidal gold probes to tag macromolecules provides another means for identifying specific molecules in complex systems. The motions of gold-tagged molecules have generally been quantitated using video microscopy to measure the single particle absorbance of the gold and to track single particles in each image. Correlation techniques have been applied to data obtained from video microscopy for population measurements of gold particle motion (de Brabender et al., 1991), but the temporal resolution was limited by the time needed to collect an entire

Received for publication 13 October 1992 and in final form 4 October 1993.
Address reprint requests to Dennis E. Koppel, Department of Biochemistry, University of Connecticut Health Center, Farmington, Connecticut 06030 USA.

0006-3495/94/02/502/06 $2.00

video frame. Using the scanning confocal microscope with reflectance contrast optics provides a straightforward means to examine gold particle motions by autocorrelation techniques.

We present here two different demonstrations of scanning concentration correlation spectroscopy. First, we have used scanning FCS to study motions of DNA molecules, stained with ethidium bromide, in solution. Second, we used reflectance contrast microscopy to examine the motions of colloidal gold-tagged lipids in planar bilayers.

MATERIALS AND METHODS

Confocal Microscopy

Confocal microscopy was performed with a BioRad (Richmond, VA) MRC 600 laser scanning system attached to a Zeiss (Thornwood, NY) Axioskop, equipped with a Nikon (Melville, NY) 60×, 1.4 N.A. oil immersion objective, with the photomultiplier tube operating in the analog mode. Ethidium bromide-stained DNA and fluorescent beads were analyzed using the BHS filter block (excitor filter 488 DF 10, dichroic reflector 510 LP, emission filter OG 515 LP). 40-nm gold particles were analyzed by reflectance contrast, where the sample was illuminated with incident laser light using a half-silvered mirror with no additional optical elements.

The basic method of data collection was to repeatedly scan a single line of 768 pixels across the specimen. The line scan was repeated 512 times, and each line of data was stored as a single line of a 512 × 768 digital image. Thus, data from a single experiment consists of an "image" file, in which the spatial component (x) is displayed on the horizontal axis and the temporal component (t) is displayed on the vertical axis (see Fig. 1 *A*, *C*, and *E* and Fig. 2 *B* and *E*, for examples). Data was collected with different settings of the confocal aperture. This changes the size of the observation volume and is analogous, in some respects, to changing the beam size in a conventional FCS experiment. Sequential line scanning of 768 pixels per line was performed using the MRC software version 4.62. The dimensions of the area scanned can be varied by changing the incremental deflection of the scanning mirror (with the MRC-600 software this is accomplished by using the "zoom" command). At the fastest scan rate, one line of 768 pixels is scanned in 1/512 s (1.95 ms); at the slowest scan rate, one line of 768 pixels is scanned in 3/512 s (5.86 ms). The interval between sequential scan lines was varied by accumulating multiple laser passes into a single line of data. So for instance, a whole run that takes a total of 30.0 s can consist of [(a slow scan line of 3/512 s) × (10 laser passes)] × (512 times) = 30.0 s.

Computer Analysis

For FCS, a value of uncorrected optical intensity at coordinate x and time t, $I_u(x, t)$, is corrected as

$$I(x, t) = \frac{I_u(x, t) - I_0}{I_d(x) - I_0(x)}, \tag{1}$$

where subscripts 0 and d signify the dark current and a concentrated dye solution, respectively, as described by Koppel et al., 1989. The conversion from $I_u(x, t)$ to $I(x, t)$ for gold-labeled samples is corrected as

$$I(x, t) = I_u(x, t) - N^{-1} \sum_n I_u(x, t_n). \tag{2}$$

For gold-labeled lipid bilayers the summation covers N points in which the only gold particles appearing are immobile. For the case of aqueous suspensions of particles, the summation covers all the points.

A network connection that links the confocal PC and a Silicon Graphics Computer (IRIS 4D-340 VGX Graphics Workstation, Mountain View, CA) carries the data as separate precorrelation files. After the raw data is corrected according to Eq. 1 or 2, the correlation function is computed as

$$g(n\Delta x, m\Delta t) = \frac{\sum_n \sum_m I(x, t) I(x+n\Delta x, t+m\Delta t)}{\langle I \rangle^2} - 1. \tag{3}$$

The computed correlation function was approximated by a fit to the following curve (MLAB Mathematical Modeling program, Civilized Software, Bethesda, MD)

$$g(n\Delta x, m\Delta t) = A \frac{\exp[-(n\Delta x/W)^2/(1 + m\Delta t/\tau)]}{1+m\Delta t/\tau + B}, \tag{4}$$

based on a two-dimensional Gaussian laser profile. The two-dimensional theory, as opposed to some three-dimensional function that takes into account diffusion along the optical axis, is expected to mimic the behavior with only minor error (See, Qian and Elson, 1991). Equation 3 was derived by replacing the position of the particle with a Gaussian of dimension a_0^2, giving a coefficient W approximately equal to

$$W^2 = (w_0^2 + a_0^2) \tag{5}$$

where w_0 is the effective beam radius in two dimensions at the $1/e^2$ points. The diffusion coefficient D is inversely proportional to time constant τ. To calculate the diffusion coefficient from the data, we apply the following formula

$$D = \frac{W^2}{4\tau}. \tag{6}$$

Coefficient A in Eq. 4 is equal to one over the number of particles in the three dimensional volume, and B adds a small constant to the fitting procedure. The number of particles is perhaps one of the most important parameters that one can get by this method (Weissman et al., 1976; Petersen, 1986a, b).

Sample Preparation

Linear, double stranded Herpes simplex virion DNA (HSV-1 strain KOS grown in VERO cells), purified by a gentle method to avoid shearing (Zhu and Weller, 1988), was obtained from A. Malik (University of Connecticut Health Center, Farmington, CT). The size of the DNA was 152 kb. Linear double stranded plasmid DNA (pKS, 5.0 kb) was obtained from K. Ainger (University of Connecticut Health Center, Farmington, CT).

DNA was stained with ethidium bromide (0.1 μg/ml) in water (LePecq and Paoletti, 1967). For FCS, DNA was loaded into a rectangular microcapillary (1.0 × 0.05 mm^2 microslide, Vitrodymics, Rockaway, NJ), which was sealed onto a microscope slide for examination. Correlation functions were also obtained using fluorescent microspheres (0.5 μm diameter, Polysciences, Inc., Warrington, PA).

Supported planar bilayers were prepared from liposomes composed of egg phosphatidylcholine (Sigma Chemical Co., St. Louis, MO), cholesterol (Avanti Polar Lipids, Birmingham, AL), and biotinylated phosphatidylethanolamine (Molecular Probes, Eugene, OR) in a molar ratio of 500:100:1 as described by Lee et al. (1991). Avidin-labeled colloidal gold was prepared by adding 500 μl of 40-nm colloidal gold (EY Laboratories, San Mateo, CA) to 500 μl of 1 mg/ml-avidin (Neuralite Avidin, Molecular Probes) in phosphate-buffered saline (PBS) or 1 mg/ml bovine serum albumin (BSA) (Fraction V, Sigma) and incubating for 30 min at 4°C. The gold was centrifuged at 12,000 × g for 10 min and resuspended by sonication in 1 ml 0.5% BSA and 0.5% Carbowax in PBS. After three washes in the BSA/carbowax solution, the final pellet was resuspended in 100 μl PBS. The avidin-gold was stored at 4°C for up to 1 week. Before use the gold was washed once in 0.5% BSA in PBS and sonicated into suspension.

The planar bilayers were washed with 0.5% BSA in PBS, and avidin-gold or BSA-gold was added. After incubation for 15 min at room temperature, the unbound gold was removed by washing with 0.5% BSA in PBS, as described by Lee et al. (1991), and the chamber was sealed with valap. For a control, colloidal gold was used directly as it came from the manufacturer.

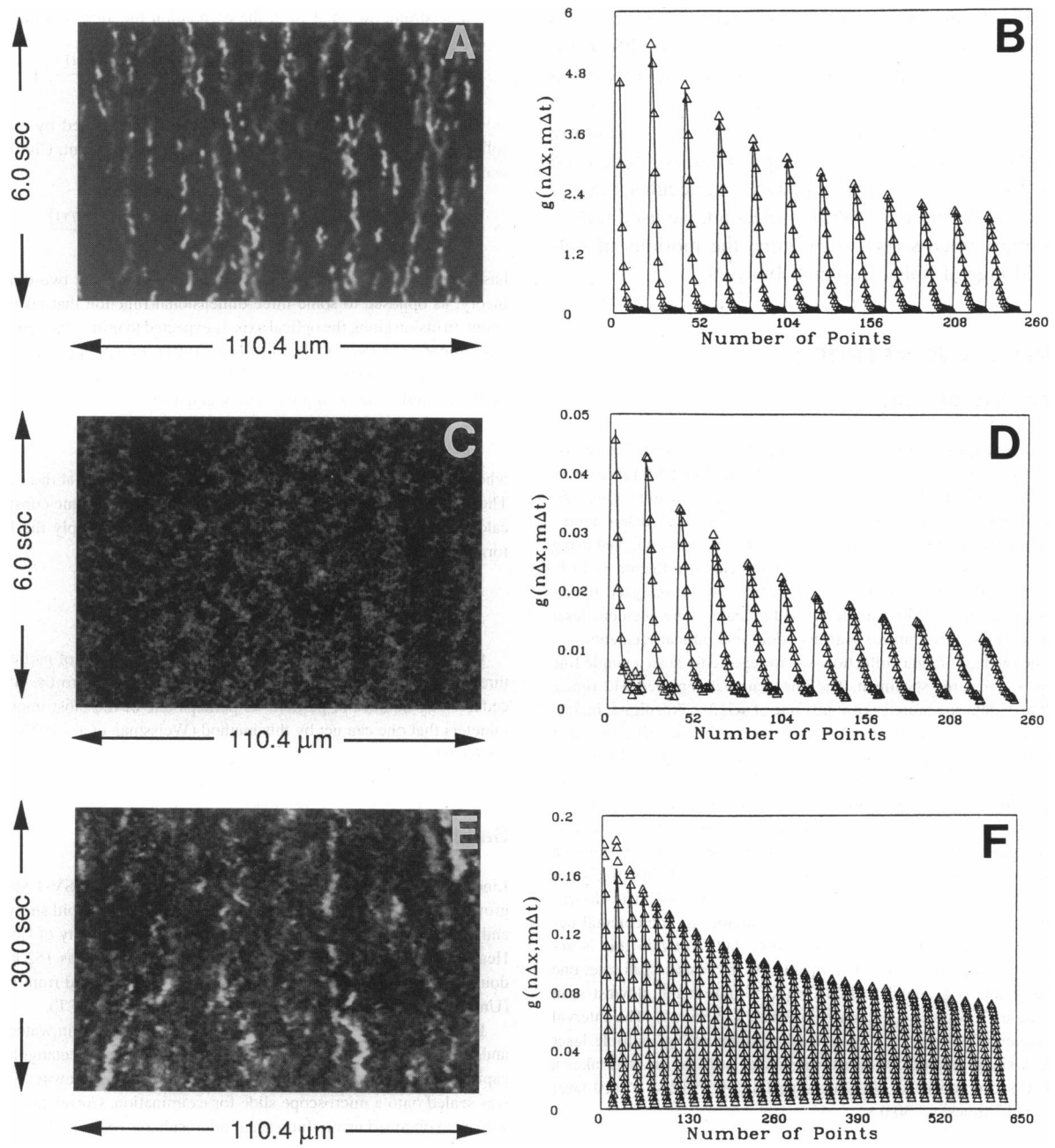

FIGURE 1 SCCS of fluorescent beads and DNA. Panels *A*, *C*, and *E* show raw data files from single runs presented in precorrelation scan files. A single line scan of 768 pixels is repeated 512 times, and each sequential scan is displayed vertically to generate the scan files. All the runs show data collected with a confocal aperture of 5.10 mm. Panels *B*, *D*, and *F* show the correlation functions, as a function of space and time, averaged over five separate experiments with a confocal aperture of 5.10 mm. *A* and *B*, data for 0.5-μm diameter polyspheres; *C* and *D*, data for pKS DNA; and *E* and *F*, data for HSV DNA.

RESULTS

Assessment of the scanning concentration correlation spectroscopy (SCCS) method using fluorescent microspheres

Use of the confocal laser scanning microscope for FCS was initially characterized using 0.5-μm diameter fluorescent polyspheres. For each sample, we recorded five scan files, at each of three confocal apertures. Fig. 1*A* shows the raw data file from a single run in a precorrelation data file, for one intermediate beam size. This data file consists of consecutive single line scans displayed vertically, and thus looks similar to a video image. The short vertical squiggles in the scan files correspond to the appearance of one or more particles or molecules in sequential scans. Fig. 1*B* shows the corresponding average correlation function as a function of space and time. The smooth curve represent the theoretical fit. mΔt and nΔx are the incremental changes in time and space. Note that two points from the zero time correlation function are deleted as shot noise arising during the detection process for the analogue photocurrent. Table 1 gives the coefficients from the theoretical curves for each experiment. Fitting the data to more than one confocal aperture is analogous, in some respects,

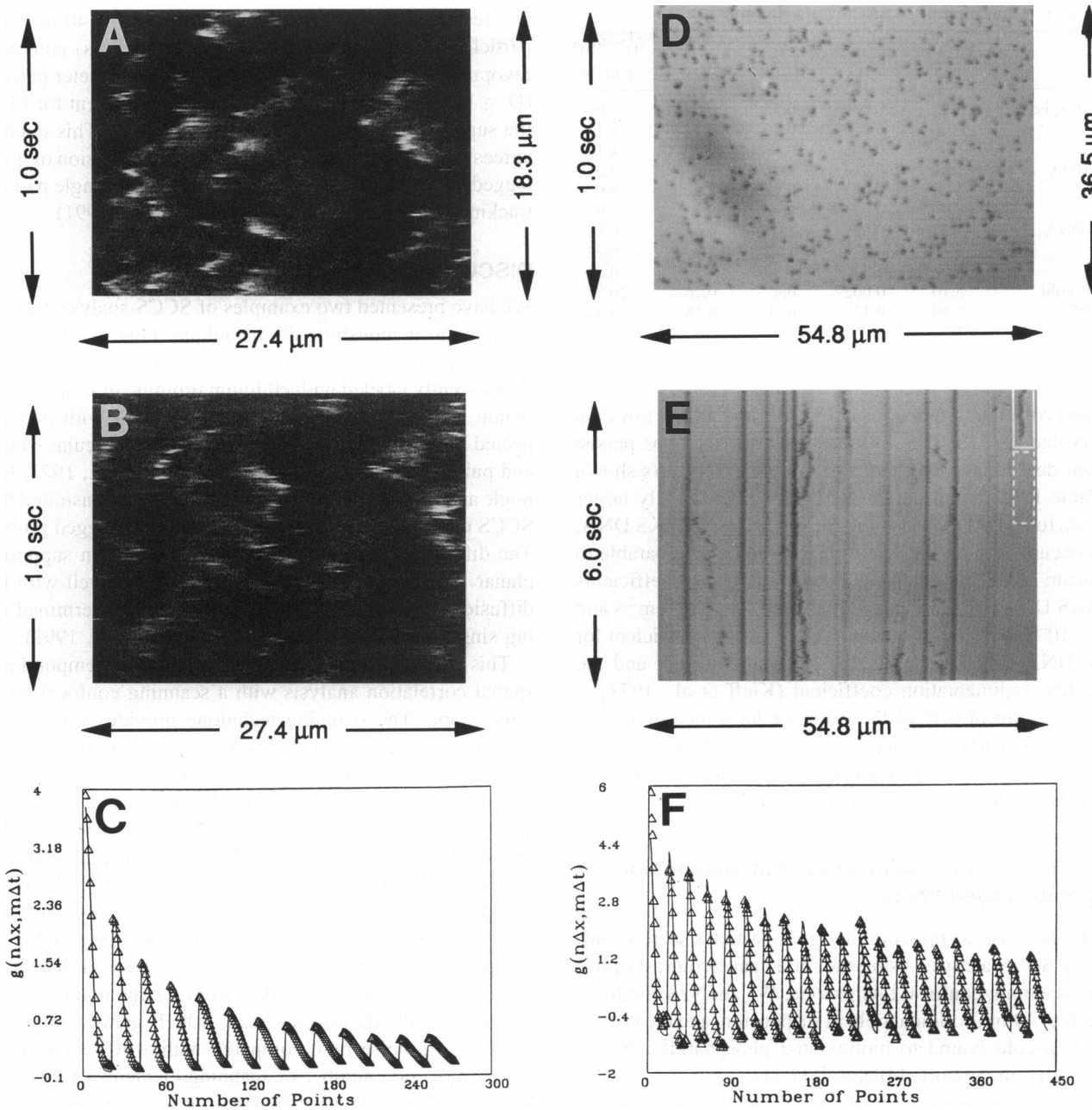

FIGURE 2 SCCS of 40-nm colloidal gold in suspension and gold-labeled PE in supported bilayers. Panel *A* shows a two dimensional reflectance contrast image of colloidal gold in suspension as a function of x and y. The time axis to the right of the figure shows the time required to scan a full image. The image was collected with a confocal aperture of 8.10 mm, and the zoom was set such that the line scanned is 27.4 μm in the horizontal axis. Panel *B* shows a raw data file taken with the same confocal aperture and horizontal scan distance as *A*, and panel *C* shows the correlation function averaged over 10 separate experiments for confocal aperture of 5.01 mm and horizontal scan distance of 54.8 μm. Panel *D* shows a two dimensional reflectance contrast image of gold-labeled PE in a supported bilayer, taken with a confocal aperture of 5.01 mm and a horizontal setting of 54.8 μm. Panel *E* presents a raw data file for gold-labeled PE in a supported bilayer taken at the same confocal aperture and horizontal settings as *D*. The *boxes* shown in *E* represent an example of a portion of the data chosen for analysis. The *solid box* shows a region containing a mobile particle chosen for analysis, and the *dashed box* shows the region used as a background. Panel *F* shows the correlation function for gold-labeled PE averaged over ten separate particles, at confocal aperture of 5.01 mm and horizontal setting of 54.8 μm.

to fitting the data with more than one beam size. Note that D is independent of the confocal aperture. However the signal-to-noise ratio decreases as the confocal aperture decreases. The theoretical diffusion coefficient calculated for a 0.5-μm diameter sphere is 9.3×10^{-9} cm^2/s, which is within a factor of 0.8 of the experimentally measured coefficient for the particle.

FCS analysis of DNA in solution

We next used the method to determine the average diffusion coefficient for different sizes of DNA molecules stained with ethidium bromide. Raw data files, and the corresponding theoretical curves, for pKS DNA and HSV DNA are shown in Fig. 1 *C* and *E*, respectively, and the corresponding

TABLE 1 Coefficients of SCCS Experiments

	Pinhole (mm)	τ (s)	W (μm)	1/A	D × 10^8 (cm^2/s)
0.5 μm spheres	1.27	0.039	0.41	0.098	1.09
	5.10	0.053	0.50	0.12	1.19
	8.0	0.085	0.63	0.55	1.17
pKS DNA	1.27	0.028	0.61	6.8	3.3
	5.10	0.032	0.71	12.3	4.0
	8.0	0.073	1.06	59.3	3.9
HSV DNA	1.27	0.52	1.07	4.0	0.56
	5.10	0.97	1.11	4.7	0.32
	8.0	1.34	1.37	7.2	0.35
40-nm gold	5.10	0.0027	0.47	0.26	20.8
gold-PE	5.10	0.12	0.48	0.18	0.46

average correlation functions in Fig. 1 *D* and *F*. The raw data shows that the HSV DNA fluorescence correlations persist a great deal longer than those of the pKS DNA. As shown in Table I, the beam parameter (W) is significantly larger than w_0 for HSV DNA (see Eq. 5), and less so for pKS DNA. This occurs because the size of HSV DNA is comparable to the beam size. This gives the average diffusion coefficients for pKS DNA and HSV DNA of about 3.7×10^{-8} cm^2/s and 4.1×10^{-9} cm^2/s, respectively. The diffusion coefficient for HSV DNA calculated from the molecular weight and the published sedimentation coefficient (Kieff et al., 1971) is within a factor of 0.75 of the value we have measured. The diffusion coefficient measured for pKS DNA is also comparable to diffusion coefficients calculated for similar sized DNA molecules (Icenogle and Elson, 1983a, b).

SCCS analysis of colloidal gold in suspension and gold-tagged lipids

The motions of 40-nm colloidal gold particles were examined by SCCS analysis using the reflectance contrast optics of the scanning confocal microscope. We analyzed both the motion of 40-nm colloidal gold in suspension, and the motion of avidin-gold bound to biotinylated phosphatidylethanolamine (PE) in supported planar bilayers.

Fig. 2 *A* and *D* show static, two dimensional images of 40-nm gold in suspension and the avidin-gold bound to the supported planar bilayers, respectively. In control experiments, BSA-gold did not bind to bilayers containing biotinylated PE, nor did avidin-gold bind to bilayers lacking biotinylated PE (data not shown). Note that the gold bound to the membrane appears darker than the gold in suspension because of some kind of interference effect.

Raw data files for gold in suspension and gold-labeled PE in planar bilayers are shown in Fig. 2 *B* and *E*, respectively. The boxes superimposed on Fig. 2 *E* represent an example of a portion of the data chosen for analysis. The *solid box* contains the raw data, and the *dashed box* contains the corresponding background (See Eq. 2). For gold-labeled lipid bilayers the summation for the background only covers points in which the only gold particles appearing are immobile. All other types of experiments use all of the data.

Fig. 2 *C* and *F* show the corresponding average correlation functions for colloidal gold, in suspension and on PE bilayers, respectively. The diffusion coefficient for 40-nm gold particles in suspension ($D = 2.1 \times 10^{-7}$ cm^2/s) compares favorably with that calculated for a 40-nm diameter particle ($D = 1.1 \times 10^{-7}$ cm^2/s). The diffusion coefficient for PE in the supported bilayers was 4.6×10^{-9} cm^2/s. This number agrees very well with measurements of the diffusion of gold-tagged PE in similar preparations obtained by single particle tracking ($D = 2.6 \times 10^{-9}$ cm^2/s; Lee et al., 1991).

DISCUSSION

We have presented two examples of SCCS analysis that are intended to demonstrate the technique. First, we have presented an FCS analysis of the motion of DNA molecules, fluorescently labeled with ethidium bromide in solution. We obtain diffusion coefficients that agree well with that expected based on calculation of D from the molecular weight and published sedimentation values (Kieff et al., 1971; Icenogle and Elson, 1983*b*). Second, we have demonstrated that SCCS can be used to examine colloidal gold tagged probes. The diffusion coefficient for gold-labeled PE in supported planar membranes obtained by SCCS agrees well with the diffusion coefficient of similar preparations determined using single particle tracking methods (Lee et al., 1991).

This work describes a procedure to perform temporal and spatial correlation analysis with a scanning confocal laser-microscope. The scanning technique provides several improvements when compared with a conventional FCS experiment. First of all, it uses the scanning capabilities of the microscope to obtain spatial information that is needed to interpret the correlation function (For comparison, see the discussion of the scanning photobleaching experiment (Koppel, 1979)). For particles of a size comparable to the wavelength of light, the scanning capability gives a measure of the particle size over and above the beam size (see Eq. 5), comparable to light scattering as a function of scattering angle. Secondly, it collects data from a large number of independent subvolumes per scan, which greatly improves the signal-to-noise ratio compared with a FCS experiment with a moderate number of scanning elements (Meyer and Schindler, 1988). Third, there are improvements provided by the confocal microscope itself (see Qian and Elson, 1991). These include the improved signals, and signal-to-noise ratio, associated with the subcellular confocal beam size. Finally, this methodology can be used for nonfluorescent probes such as colloidal gold, by using the reflectance mode of the microscope.

The measurable diffusion rates by SCCS are limited by the scan rate of the instrument, unless one restricts the resolution, say by limiting the laser light to the center of the objective. The measurement conditions we have used are such (60x, 1.4 N.A. objective, confocal aperture 8.0 mm, 1/512 ms between scans) that they limit the MRC 600 to measurable diffusion rates of less than 1×10^{-7} cm^2/s. We have measured diffusion of 40-nm colloidal gold particles in suspension to be 2.1×10^{-7} cm^2/s, demonstrating that measurements on this order are easily obtained. Other commercially available systems can scan at higher scan rates (video rates of 30 frames/s), so this limitation can be overcome.

Fig. 2 *D* shows a static, two dimensional image of the avidin-gold bound to the supported planar bilayers. In contrast, Fig. 2 *A* shows a two dimensional image of the 40-nm colloidal gold in suspension that is anything but static, even though the MRC 600 is scanning at the fastest speed possible. For comparison see Fig. 2 *B* and *E*, which show one dimensional scan files of the colloidal gold in suspension and membrane-bound. The two dimensional image of the gold in suspension looks more like the one dimensional scan file rather than a static image, because the scan rate used for obtaining two dimensional images with the MRC-600 is slow relative to the motions of the particles. It is possible to do a correlation analysis on a two dimensional scanned image, such as that shown in Fig. 2 *A*, that incorporates both x and y spatial components and a temporal component. This type of analysis would be particularly useful for SCCS analysis using living cells, in that the entire cell could then be used for analysis. Unfortunately, the software currently available for the MRC 600 does not allow collection of two dimensional images while varying the interval between sequential scan lines.

The method of data analysis we have used for SCCS makes it straightforward to examine different regions of the observation volume for separate analysis. For more complicated data it is possible to inspect an entire raw data file and isolate particular regions of the "image" for separate analysis, as was done for the membrane-bound gold for example. In more complicated SCCS data analysis, just as in single scan line data, one can partition the pixels in the raw data image file into subsets of different images. These can be used to get an image of a single cell placed in more than one type of environment, or to analyze diffusion subregions within a single cell.

In addition to the single channel method of FCS we have discussed, it is also possible to use a second fluorescence channel, optional with most instruments, to obtain a second fluctuation signal. One can then analyze the data as three correlation signals, two auto-correlation signals and a cross-correlation signal. From the signal amplitudes one can obtain anywhere from 0 (indicating no interaction between the two fluorescent species) to 1 (indicating complete correlation between the two fluorescent species) in weighting of the two channels. Two-channel FCS data should make it possible to observe changes in interactions between molecules under different experimental situations and is potentially applicable to measuring molecular interactions in the cytoplasm of the living cell.

We gratefully acknowledge support from the United States Public Health Service under grants GM23585 and ES05973 to D.E.K. and grant NS15190 to J.H.C.

REFERENCES

1. de Brabender, M., R. Nuydens, A. Ishihara, B. Holifield, K. Jacobson, and H. Geerts. 1991. Lateral diffusion and retrograde movements of individual cell surface components on single motile cells observed with Nanovid microscopy. *J. Cell Biol.* 112:111–124.
2. Elson, E. L., and D. Magde. 1974. Fluorescence correlation spectroscopy, I. Conceptual basis and theory. *Biopolymers.* 13:1–27.
3. Icenogle, R. D., and E. L. Elson. 1983*a*. Fluorescence correlation spectroscopy and photobleaching recovery of multiple binding reactions. I. Theory and FCS measurements. *Biopolymers.* 22:1919–1948.
4. Icenogle, R. D., and E. L. Elson. 1983*b*. Fluorescence correlation spectroscopy and photobleaching recovery of multiple binding reactions. II. FPR and FCS measurements at low and high DNA concentrations. *Biopolymers.* 22:1949–1966.
5. Kieff, E. D., S. L. Bachenheimer, and B. Roizman. 1971. Size, composition, and structure of the deoxyribonucleic acid of Herpes Simplex Virus subtypes 1 and 2. *J. Virol.* 8:125–132.
6. Koppel, D. E. 1974. Statistical accuracy in fluorescence correlation spectroscopy. *Phys. Rev. A.* 10:1938–1945.
7. Koppel, D. E. 1979. Fluorescence redistribution after photobleaching: a new multipoint analysis of membrane translational dynamics. *Biophys. J.* 28:281–291.
8. Koppel, D. E., D. Axelrod, J. Schlessinger, E. L. Elson, and W. W. Webb. 1976. Dynamics of fluorescence marker concentration as a probe of mobility. *Biophys. J.* 16:1315–1329.
9. Koppel, D. E., Carlson, C., and Smilowitz, H. 1989. Analysis of heterogeneous fluorescence photobleaching by video kinetics imaging: the method of cumulants. *J. Microsc. (Oxford)* 155: Pt2, 199–206.
10. Lee, G. M., A. Ishihara, and K. A. Jacobson. 1991. Direct observation of Brownian motion of lipids in a membrane. *Proc. Natl. Acad. Sci. USA.* 88:6274–6278.
11. LePecq, J.-B., and C. Paoletti. 1967. A fluorescent complex between ethidium bromide and nucleic acids. Physical-chemical characterization. *J. Mol. Biol.* 27:87–106.
12. Magde, D., E. L. Elson, and W. W. Webb. 1974. Fluorescence correlation spectroscopy, II. An experimental realization. *Biopolymers.* 13: 29–61.
13. Meyer, T., and H. Schindler. 1988. Particle counting by fluorescence correlation spectroscopy. Simultaneous measurement of aggregation and diffusion of molecules in solutions and in membranes. *Biophys. J.* 54:983–993.
14. Nicoli, D. F., J. Briggs, and V. B. Ellings. 1980. Fluorescence immunoassay based on long time correlations of number fluctuations. *Proc. Natl. Acad. Sci. USA.* 77:4904–4980.
15. Palmer, A. G., and N. L. Thompson. 1987*a*. Theory of sample translation in fluorescence correlation spectroscopy. *Biophys. J.* 51: 339–343.
16. Palmer, A. G., and N. L. Thompson. 1987*b*. Molecular aggregation characterized by high order autocorrelation spectroscopy. *Biophys. J.* 52:257–270.
17. Petersen, N. 0. 1986*a*. Scanning fluorescence correlation spectroscopy. I. Theory and simulation of aggregation measurements. *Biophys. J.* 49:809–816.
18. Petersen, N. O. 1986*b*. Scanning fluorescence correlation spectroscopy, II. Application to virus glycoprotein aggregation. *Biophys. J.* 49: 817–820.
19. Petersen, N. O., and E. L. Elson. 1986. Measurements of diffusion and chemical kinetics by fluorescence photobleaching recovery and fluorescence correlation spectroscopy. *Methods Enzymol.* 130:454–484.
20. Petersen, N. O., P. L. Hoddelius, P. W. Wiseman, O. Seger, and K.-E. Magnusson. 1993. Quantitation of membrane receptor distributions by Image Correlation Spectroscopy: concept and application. *Biophys. J.* 65:1135–1146.
21. Thompson, N. L., and D. Axelrod. 1983. Immunoglobulin surface-binding kinetics studied by total internal reflection with fluorescence correlation spectroscopy. *Biophys. J.* 43:103–114.
22. Qian, H., and E. L. Elson. 1991. Analysis of confocal laser-microscope optics for 3-D fluorescence correlation spectroscopy. *Appl. Optics.* 30: 1185–1195
23. Weissman, M., H. Schindler, and G. Feher. 1976. Determination of molecular weights by fluctuation spectroscopy: application to DNA. *Proc. Natl. Acad Sci. USA.* 73:2776–2780.
24. Zhu, L., and S. K. Weller. 1988. UL5, a protein required for HSV DNA synthesis: genetic analysis over expression in Escherichia coli and generation of polyclonal antibodies. *Virology* 166:366–378.